ACS APPLIED MATERIALS & INTERFACES

Research Article

www.acsami.org

Optimizing the Mass-Specific Activity of Bilirubin Oxidase Adlayers through Combined Electrochemical Quartz Crystal Microbalance and Dual Polarization Interferometry Analyses

Trevor McArdle,[†] Thomas P. McNamara,[†] Fan Fei,[†] Kulveer Singh,[†,‡] and Christopher F. Blanford*[,†]

[†]School of Materials and Manchester Institute of Biotechnology, University of Manchaster, 131 Princess Street, Manchester M1 7DN, United Kingdom

[‡]Department of Chemistry, Inorganic Chemistry Laboratory, University of Oxford, South Parks Road, Oxford OX1 3QR, United Kingdom

Supporting Information

ABSTRACT: Two surface analysis techniques, dual polarization interferometry (DPI) and analysis by an electrochemical quartz crystal microbalance with dissipation capability (E-QCM-D), were paired to find the deposition conditions that give the highest and most stable electrocatalytic activity per adsorbed mass of enzyme. Layers were formed by adsorption from buffered solutions of bilirubin oxidase from *Myrothecium verrucaria* at pH 6.0 to planar surfaces, under high enzyme loading (≥1 mg mL^{-1}) for contact periods of up to 2 min. Both unmodified and carboxylate-functionalized gold-coated sensors showed that a deposition solution concentration of 10−25 mg mL^{-1} gave the highest activity per mass of adsorbed enzyme with an effective catalytic rate constant (k_{cat}) of about 60 s^{-1}. The densification of adsorbed layers observed by DPI correlated with reduced bioactivity observed by parallel E-QCM-D measurements. Postadsorption changes in thickness and density observed by DPI were incorporated into Kelvin−Voigt models of the QCM-D response. The modeled response matched experimental observations when the adlayer viscosity tripled after adsorption.

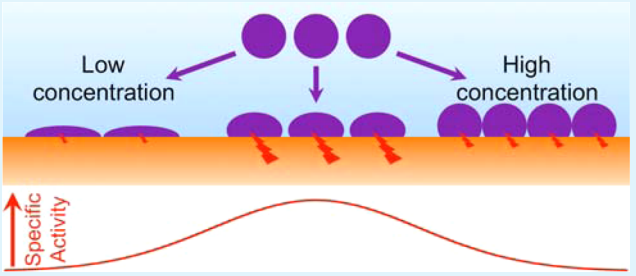

KEYWORDS: *enzymatic biofuel cell, industrial biotechnology, protein immobilization, protein−surface interactions, laccase, multicopper oxidase*

INTRODUCTION

Enzymes used in biotechnological processes are often immobilized to create heterogeneous catalysts that are readily isolated from a reaction mixture.[1,2] A persistent challenge in enzyme immobilization is maintaining catalytic activity in spite of energetic and steric effects that render some of the immobilized enzyme inactive or ineffective.[3] For example, a protein may spread and denature on adsorption or be oriented so that access to substrate binding sites is blocked.[4,5] The situation is more complex in bioelectrocatalytic systems: oxidoreductases, enzymes that catalyze electron-transfer reactions, must also be encapsulated or positioned in a way that ensures that electron transfer does not limit the overall reaction rate.[6−8] Solutions to these challenges include entrapment of enzyme in hydrogels containing tethered electron-transfer mediators that surround the enzyme[9] and the use of substrate mimics to orient and stabilize enzymes.[10]

This study follows from observations in our lab that the most stable and active enzyme adlayers were formed from concentrated protein solutions, often in excess of 10 mg mL^{-1}. Here we present a systematic investigation into the origin of these observations using bilirubin oxidase from *Myrothecium verrucaria* (*Mv*BOx), a 64 kDa multicopper oxidase (MCO). MCOs are a family of copper-containing enzymes that includes laccases, ascorbate oxidase, and ceruloplasmin and can catalyze the four-electron reduction of O_2 to water with a higher thermodynamic efficiency (lower overpotential) than platinum.[11,12] For this reason, MCOs have been extensively researched as real or inspirational catalysts for cathodes in low-temperature fuel cells.[7,8,13]

Bilirubin oxidase contains four copper atoms in two active sites. Dioxygen is reduced to water at a buried trinuclear cluster of copper ions. Electrons for this reduction enter the enzyme through a lone type 1 copper separated from the protein's surface by a single histidine residue. In nature, these electrons are typically supplied by the oxidation of organic substrates or ferrous iron.[14] When bilirubin oxidase is immobilized on an electrode, the lone copper needs to be no more than 1−2 nm from the electrode surface to avoid interfacial electron transfer being the rate-limiting step in oxygen-reduction electrocatalysis.[15,16] Therefore, to obtain the highest current density

Received: August 7, 2015
Accepted: October 27, 2015
Published: October 27, 2015

DOI: 10.1021/acsami.5b07290
ACS Appl. Mater. Interfaces 2015, 7, 25270−25280

for a given amount of enzyme, enzyme adsorption must promote correct orientation.

Larger proteins do not behave like rigid particles and deform on adsorption depending on enzyme structure, pH, temperature, protein concentration, and surface chemistry.[4,5,7,17] For example, Pankratov et al. compared laccase and bilirubin oxidase adsorbed onto bare gold surfaces.[7] They observed laccase to be completely catalytically inactive, even after direct addition of an electron donor, suggesting rapid enzyme denaturation upon adsorption. Bilirubin oxidase showed a similar turnover frequency for the adsorbed enzyme as for the enzyme in solution. However, the catalytic activity dropped to less than 50% in only 3 h, which they attributed to conformational changes of the enzyme.

Although many studies exist for the adsorption of model proteins such as lysozymes and albumins, publications on how adsorption affects biocatalytic function are rarer. Herrera et al. investigated the surface coverage of D-amino acid oxidase and its relationship to surface bioactivity.[18] Surface filling and relaxation times of the adsorbing protein were monitored for different experimental conditions using in situ amperometry and ex situ spectrophotometry. On silica, the relaxation step occurred at the same rate of surface filling when the substrate and enzyme were oppositely charged. For unfavorable electrostatic conditions, the relaxation time occurred over a larger time. Bioactivity was irrespective of the surface coverage in both cases. Adsorption to gold showed that the relaxation step was driven by hydrophobic interactions and highly dependent on surface coverage. Therefore, surface activity was only maintained at high surface coverages.

Surface modifiers such as organothiols and organosilanes offer a straightforward method to control the surface chemistry of electrodes. Long-chain alkylthiols, in particular, can produce highly organized self-assembled monolayers (SAMs), allowing the terminal groups to change the properties of the surface.[19,20] Tominaga and co-workers used SAMs on Au(111) electrodes to establish that the electron transfer to *Mv*BOx is fastest on negatively charged surfaces.[21] Olejnik et al. studied laccase adsorption on functionalized gold electrodes of phenyl groups ending with aminoethyl or carboxyethyl entities.[6] In this case, the aminoethyl functionality increased the oxygen reduction activity of laccase. This was ascribed to the closer proximity of the T1 site to the electrode. Singh et al. investigated physical adsorption and covalent attachment of *Mv*BOx onto carboxylate-terminated SAMs. They showed how rapid enzyme deactivation occurred during cycling of the potential and that covalent attachment failed to increase activity or stability.[8] Ulyanova et al. evaluated immobilization methods for two MCOs by comparing the catalytic response in the presence and absence of an electron-transfer mediator.[22] An increase in current in the presence of mediator reported on how much adsorbed enzyme remained catalytically competent but unfavorably oriented for direct electron transfer from the multiwall carbon nanotube electrode.

An electrochemical quartz crystal microbalance with dissipation analysis (E-QCM-D) is a device that can simultaneously measure adsorbed mass (through a drop in resonant frequency), provide information on layer rigidity (through the rate of dissipation of stored energy in the resonator), and quantify catalytic activity (through electrochemical measurements).[23] The E-QCM-D probes the hydrated mass of the adsorbed layer due to coupling of water within and around the proteins.[24] Dissipation is a measurement of how much vibrational energy from the oscillating crystal is lost per cycle.[25] Energy loss relays information about the rigidity of the adsorbed layer and how its changes with time, i.e., structural changes or dehydration.[26] The addition of electrochemical measurements provides a way to simultaneously assay catalytic competence in adsorbed oxidoreductases.[23]

Dual polarization interferometry (DPI) complements E-QCM-D measurements by probing the dry mass of an adlayer.[27] An adlayer on a sensing waveguide changes its effective refractive index (RI), shifting the phase intensity of light propagating through it relative to a reference waveguide. The use of two polarizations of incident light allows the thickness and refractive index to be resolved and from there, the density, mass and thickness of the adlayer can be calculated.[28]

Studies combining the QCM with similar optical techniques such as surface plasmon resonance (SPR) can give complementary hydrated and dry adsorbed masses of proteins. Caruso et al.[29] showed the advantage of using QCM with SPR to give the wet and dry mass of ferritin. However, in SPR, light of only one polarization (transverse magnetic) is used to determine the mass per unit area of adsorbed films, so SPR cannot determine both the thickness and the refractive index simultaneously.[30] There have been studies relating QCM-D to DPI,[31,32] including work from Xu and co-workers that examined lysozyme adsorption on silica surfaces from 0.5−200 μM protein solutions.[33] On the basis of calculations of fractional solvation of the adlayers, the group proposed that lysozyme formed increasingly densely packed layers accompanied by changes in protein orientations with higher protein solution concentrations. Later work from the same authors used these techniques to study surface energy effects on the adsorption of lysozyme, α-synuclein and BSA.[34] The latter two "soft" proteins were most affected by surface chemistry. QCM has also been used to study the effects of protein concentration on the adsorption of bovine serum albumin (BSA),[35] a globular protein with a size similar to that of *Mv*BOx. Although the authors did not measure dissipation directly, their controls allowed them to conclude that protein shape and function were better maintained when adsorbing from high-concentration protein solutions.

This current work follows nonequilibrium surface adsorption of *Mv*BOx to bare and SAM-modified surfaces using QCM and DPI. This study establishes how the mechanics and catalytic activity of an adlayer are affected by deposition solution concentration. The optimization method developed here can be applied to other oxidoreductases to improve the sensitivity and range of experiments available for analytical protein film electrochemistry[36] and to facilitate enzymatically catalyzed generation of fine chemicals (that is, industrial biotechnology applications) using surface-immobilized oxidoreductases.[23]

EXPERIMENTAL SECTION

Materials and Reagents. Lyophilized *Mv*BOx powder (Amano Enzyme EU, Chipping Norton, UK) was dissolved in 0.1 M sodium phosphate buffer, pH 6.0, at 4 °C. The solution was purified by centrifugation through poly(ether sulfone) membrane (Vivaspin, 30 kDa MWCO) to remove small-molecular-weight contaminants. Protein concentration was calculated by UV absorption, using ε_{280nm} = 9.52 × 10^4 M^{-1} cm^{-1}, calculated from the enzyme amino acid sequence.[37] BSA (lyophilized powder, crystallized, ≥ 98.0% Sigma-Aldrich) was dissolved in 0.1 M sodium phosphate, pH 6.0.

DOI: 10.1021/acsami.5b07290
ACS Appl. Mater. Interfaces 2015, 7, 25270−25280

Solutions of *Mv*BOx were prepared from dilutions of higher-concentration stock solutions, which were stored in the gaseous phase above liquid nitrogen. BSA solutions were freshly made up to the desired concentration and stored at 4 °C. Protein concentrations ranged from 1 to 50 mg mL^{-1} (2×10^{-5} to 8×10^{-4} M, on the basis of polypeptide mass).

The silicon oxynitride surfaces of the DPI sensors were functionalized with a 5 wt % solution of 3-(trihydroxysilyl)propane-1-sulfonic acid (THSPS, 30−35 wt % in water, Fluorochem) dissolved in ethanol. Gold surfaces were modified with 10 mM ethanolic solutions of 3-mercaptopropionic acid (3MPA, >99%, Fluka).

All further chemicals listed were used in general surface preparation and in buffers: hydrochloric acid (37%, Fisher), sodium dihydrogen orthophosphate dihydrate (99.0−101.0%, Fisher), disodium hydrogen orthophosphate anhydrous (99.5+%, Fisher), sulfuric acid (1.83 g mL^{-1}, > 95%, Fisher), hydrogen peroxide (30% w/v, Scientific Laboratory Supplies), and 3,3′-dithiobis(sulfosuccinimidylpropionate) (DTSSP, > 98%, ProChem, Inc.). Buffers were prepared from mixtures of weak acids and their complementary bases, rather than titrating with strong acid or base.

All chemicals were used as received without further purification. Water was purified via reverse osmosis and ion exchange to a resistivity of 18.2 MΩ cm at 25 °C using a Milli-Q water purifier.

Electrochemical Quartz Crystal Microbalance with Dissipation Analysis. A Q-sense E1 system was used to measure protein adsorption. For QCM-D measurements, a Q-sense flow module 401 was used (140 μL total volume, 40 μL sample chamber over sensor). The maximum mass sensitivity is 0.5 ng cm^{-2},[38,39] about 0.1−0.2% of a saturated monolayer of *Mv*BOx. E-QCM-D measurements used a modified Q-Sense QEM401 module with a 0.1 mL sample chamber volume (Supporting Information). Sensors (Q-Sense) were 14 mm diameter AT-cut quartz crystals with a fundamental frequency of 4.95 ± 0.05 MHz. Sensors were coated with gold, both with a titanium adhesion layer. The flow module and fluid handling system were positioned on an aluminum plate maintained at 25 °C using an internal water flow. The temperature of the flow module was stabilized to within 10 mK using the E1's integrated Peltier device.

QCM measurements started with a flow of buffer until a stable response was obtained, typically 30 min for the QCM-D and longer for the E-QCM-D. For E-QCM-D measurements, O_2 gas was bubbled continually through the buffer reservoir. Liquids were pulled through the cell with a peristaltic pump at 0.1 mL min^{-1}. Aliquots of *Mv*BOx solutions were introduced to the cell by pausing the flow to swap between buffer and protein solution. Time between sample loading and sensor interaction was approximately 2 min.

Adsorbed mass (typically shown as secondary *y* axes) was estimated using the Sauerbrey equation:

$$\Delta m = -\frac{C}{N}\Delta f_N \tag{1}$$

where Δm is the adsorbed mass, N is the harmonic number, Δf_N is the frequency response associated with that harmonic, and C is a proportionality constant equal to 17.9 ng cm^{-2} Hz^{-1}).

The catalytic current (i_{cat}) is proportional to both the surface coverage (Γ) and turnover frequency (k_{cat}):

$$i_{cat} = -nFA\Gamma k_{cat} \tag{2}$$

where n is the stoichiometric number of electrons transferred (4 for O_2 reduction to water), F is the Faraday constant, and A is the electrode area. The negative sign indicates reduction.

For films with low dissipation values and a constant hydrated protein mass (M_H), the ratio of catalytic current to frequency change is directly proportional to the average catalytic rate for the adsorbed enzymes (eqs 3a and 3b),[23] with a proportionality constant of 1.1×10^{-8} C s for *Mv*BOx.[8] This mass-specific catalytic activity is the key parameter for adlayer optimization.

$$\frac{i_{cat}}{\Delta f_N} = \frac{CnFA}{NM_H}k_{cat} \tag{3a}$$

$$\frac{i_{cat}}{\Delta f_N} \propto k_{cat} \tag{3b}$$

The seventh harmonic was used for data analysis. Frequency changes presented in the manuscript have not been divided by the harmonic number except where noted; this differs from the harmonic-normalized frequency response that Q-Sense software displays.

An Ivium CompactStat potentiostat was used for electrochemical measurements. A three-electrode system was used: the gold-coated QCM sensors acted as the working electrode (0.8 cm^2),[8] a 0.2 mm thick, 2.25 cm^2 rectangle of platinum located 0.7−0.8 mm from the working electrode acted as counter electrode, and a Ag/AgCl/3 M NaCl was the reference electrode (BASi RE-6, $E_{SHE} = E_{ref} + 0.21$ V).[8] Buffer was preoxygenated with industrial-grade O_2 (BOC) for at least 20 min prior to any electrocatalytic measurements. The potential for cyclic voltammetry measurements was swept between 0.7 and 0.1 V vs reference at 10 mV s^{-1}. A surface area of 0.8 cm^2 was used for current density calculations.[8]

Dual Polarization Interferometry. An *Ana*Light 4D (Farfield Group Ltd., Manchester, UK) was used to measure protein interaction with ∼1 s time resolution. The sensor chip is a dual slab, which is made of silicon oxide slightly doped with nitrogen. A HeNe 632.8 nm laser is used to illuminate the optical waveguide.

Protein was adsorbed on silicon oxynitride FB80 *Ana*Chips (dimensions 24 mm × 6 mm, Farfield Group, Ltd.) clamped inside a temperature-controlled housing. Two flow paths were defined by a fluorosilicone mask set on the chip (10 μL sensing volume, 15 mm^2 sensing area). The instrument was maintained at 25 °C. The chip surface was calibrated with bulk buffer (0.1 M sodium phosphate, pH 6.0), solutions of ethanol/water (80:20 w/w), and water, all at 25 °C. The flow rate was controlled by a mechanical syringe pump (Harvard). The injection loops were cleaned with 200 μL each of 2 wt % SDS in water, 2 wt % Hellmanex in water, and then isopropanol. Data was analyzed using *Ana*light Explorer Software (Farfield Ltd.) to calculate RI, mass, thickness, and density.

Surface Modification. Sensors for QCM and DPI were cleaned in piranha solution (3:1 v/v conc. H_2SO_4 and 30% H_2O_2) for 15 min at 80 °C. The crystal was washed with water then dried under nitrogen and exposed to UV/ozone treatment for 15 min. Bare crystals were stored for 16 h under ambient conditions before being used. Chemically modified DPI and QCM sensors were placed in the modification solution and then stored under a house nitrogen atmosphere for 16 h before being dried under nitrogen and used.

Protein Solution Viscosity and Density Measurements. Solution viscosity measurements were recorded using a AMVn Automated Microviscometer (Anton Paar). Buffered protein solutions of 1−30 mg mL^{-1} were prepared and measured twice. Intrinsic viscosity was calculated using both the Huggins and Kraemer approach. Solution densities were calculated gravimetrically using 100 and 1000 μL aliquots.

Frequency and Dissipation Modeling. Modeling the QCM-D response of the protein adlayer was based upon a Kelvin−Voigt model and used equations derived by Voinova et al.[25] and Rodahl,[40] implemented in Matlab. The introduction of the protein solution into the QCM cell was modeled as an instantaneous change from buffer to 15 mg mL^{-1} enzyme solution, then a residence time of 30 s in which the protein concentration remained constant, followed by a drop in concentration modeled as a first-order exponential with a time constant of 60 s. Enzyme absorption was modeled by the Langmuir equation using a finite-time difference method with the coverage being proportional to the average thickness. The time steps were decreased to 10 ms when convergence was observed. The density of 1450 kg m^{-3} was based on a published correlation between molecular weight and density for a 64 kDa protein.[41] The adlayer shear and viscosity values were estimated using QTools and were based upon the frequency and dissipation responses from harmonics 5, 7, and 9 for a 15 mg mL^{-1} adlayer on a 3MPA-coated sensor 15 min after adsorption. For models which described the behavior of preabsorbed layers undergoing a physical change, time constants for the increase in density and decrease in thickness were derived from the DPI analysis of *Mv*BOx

DOI: 10.1021/acsami.5b07290
ACS Appl. Mater. Interfaces 2015, 7, 25270−25280

adsorption (50 μL of 15 mg mL^{-1} *Mv*BOx) to an unmodified silicon oxynitride DPI sensor (conditions: 0.1 M sodium phosphate buffer, pH 6.0, flowing at 0.05 mL min^{-1}; 25 °C).

RESULTS AND DISCUSSION

Concentration Effects on Bare Gold and Carboxylate-Terminated Surfaces. *Adsorption on QCM Sensors.* *Mv*BOx

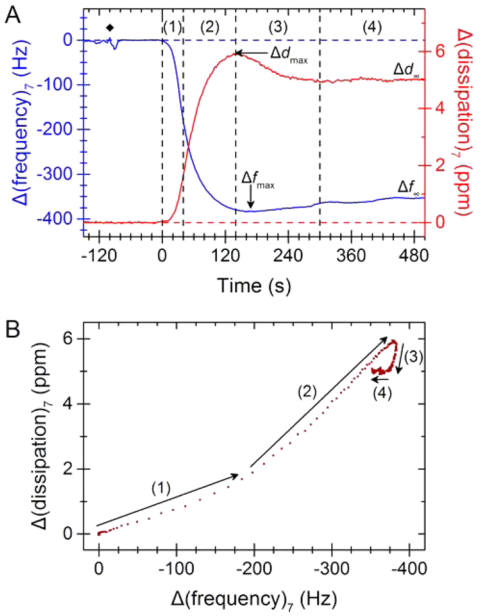

Figure 1. Typical QCM-D response for *Mv*BOx adsorbed onto a 3MPA-modified gold-coated QCM sensor. (A) Frequency and dissipation response. The black diamond indicates when the protein sample was injected into the flow system. (B) Δd vs Δf plots labeled into four distinct regions that correlate to regions of adsorption shown in A. Conditions: 0.1 M sodium phosphate buffer, pH 6.0, at 25 °C (presaturated with O_2); buffer flow rate: 0.1 mL min^{-1}; protein injection: 25 μL, 25 mg mL^{-1} *Mv*BOx; working electrode area: 0.8 cm^2; measurement temperature: 25 °C. Seventh harmonic shown.

was adsorbed on bare gold QCM sensors and gold sensors modified with the short-chain thiol 3MPA to produce a carboxylate-terminated surface. Negatively charged surfaces have been found to produce the highest electrocatalytic current for this enzyme.[21] E-QCM-D measurements were recorded for concentrations ranging from 1−50 mg mL^{-1} to follow the effect of solution concentration on adlayer properties and bioelectrocatlytic activity. A typical QCM-D response is shown in Figure 1A, where the frequency and dissipation responses are given for 25 μL of 25 mg mL^{-1} *Mv*BOx adsorbing onto a 3MPA-modified sensor.

The film-formation process consistently showed four stages that were distinguished by plotting the dissipation response (Δd) against the frequency response (Δf) (Figure 1B). To a first approximation, Δd versus Δf plots normalize the amount of energy lost from soft adlayers to their adsorbed mass.[26] Steeper slopes generally correspond to less rigidly coupled layers.

In stage 1 of the adsorption, an initial decrease in frequency (Δf) and a concomitant increase in dissipation (Δd) were observed for all concentrations investigated. This initial adsorption has been ascribed to an irreversibly bound protein layer by Rabe and co-workers in their study of β-lactoglobulin adsorption.[42] Stage 2 begins about 20−40 s after adsorption

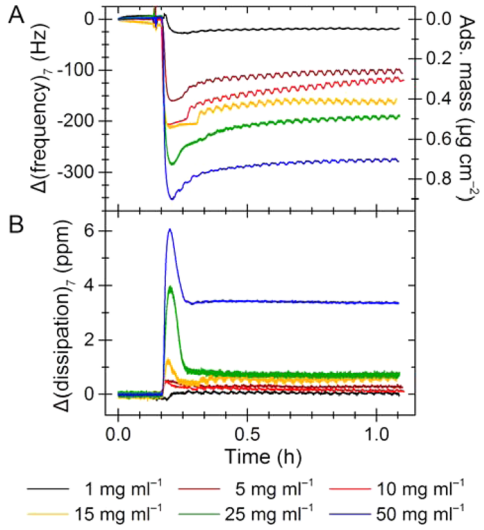

Figure 2. Effect of varying *Mv*BOx concentration on 3MPA-modified gold-coated QCM sensors. (A) QCM frequency response. (B) Dissipation response. Oscillations in the traces are from cyclic voltammetry being run. Conditions: 0.1 M sodium phosphate buffer, pH 6.0, at 25 °C (presaturated with O_2); buffer flow rate: 0.1 mL min^{-1}; protein injection volume: 25 μL; measurement temperature: 25 °C. Seventh harmonic shown. CV potential cycled between 0.91−0.31 V vs SHE at 10 mV s^{-1}.

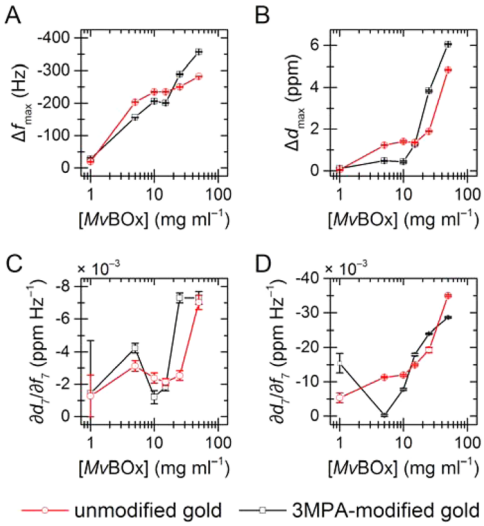

Figure 3. Summary of QCM-D analyses for *Mv*BOx adsorption to bare and 3MPA-modified gold QCM sensors, shown on semilog plots. (A) Largest magnitude frequency response (Δf_{max}) for each system, (B) maximum dissipation response (Δd_{max}), (C) $\partial d/\partial f$ value for stage 1 of adsorption, and (D) $\partial d/\partial f$ value for stage 2 of adsorption. All points are from the seventh harmonic. Error bars indicate standard error of the mean for panels A and B, and standard error of the regression for panels C and D.

and is characterized by an increase in the magnitude of $\partial d/\partial f$, indicative of the formation of a less rigid layer of protein. Stage 2 ends about 90 s after the beginning of adsorption at Δf_{max} and Δd_{max}, the highest magnitude points in the frequency and dissipation responses, respectively. The timing of the first two stages did not change with longer contact times (Supporting Information). Stage 3 is characterized by a rapid change in dissipation and a small increase for frequency (mass loss) after the response maxima. Stage 4 shows a slow decrease in the

DOI: 10.1021/acsami.5b07290
ACS Appl. Mater. Interfaces 2015, 7, 25270−25280

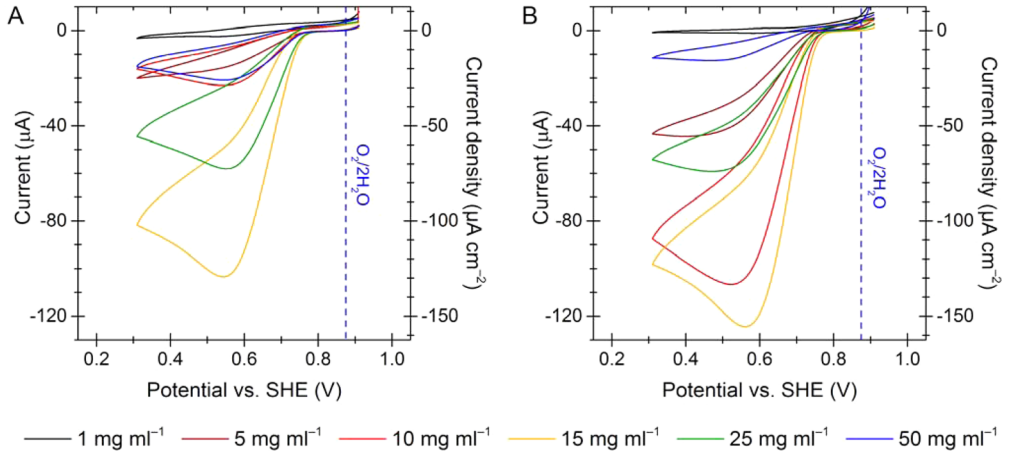

Figure 4. Electrocatalytic O_2 reduction current from adlayers of *Mv*BOx formed on gold QCM sensors: (A) unmodified and (B) 3MPA-coated. The dashed blue line indicates the thermodynamic potential for four-electron oxygen reduction. Conditions: 0.1 M sodium phosphate buffer, pH 6.0, at 25 °C (presaturated with O_2); buffer flow rate: 0.1 mL min^{-1}; protein injection volume: 25 μL; working electrode area: 0.8 cm^2; measurement temperature: 25 °C. Potential cycled between 0.91 and 0.31 V vs SHE at 10 mV s^{-1}.

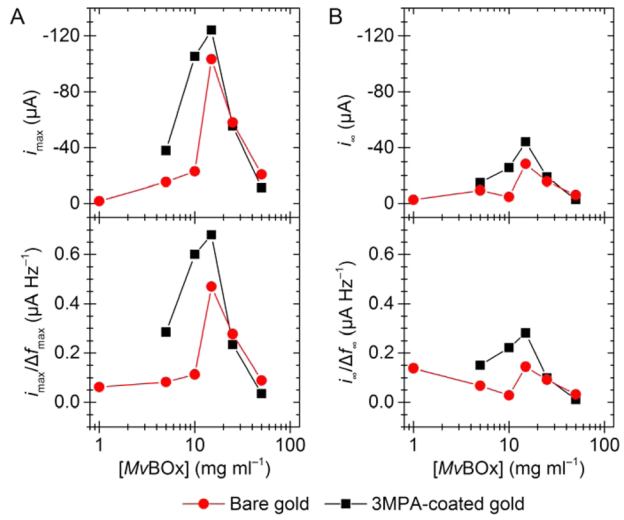

Figure 5. Electrocatalytic O_2-reduction activity of *Mv*BOx adsorbed on bare gold and 3MPA-modified QCM sensors. (A) Peak catalytic activity. (B) Catalytic activity after 25 CV cycles (50 min.). Top plots in each panel show absolute activity; bottom panels show activity normalized to the frequency change of harmonic 7, which is proportional to adsorbed mass. Activity was measured by cycling the potential between 0.91 and 0.31 V vs SHE at 10 mV s^{-1}. i_{max} was measured at 0.55 V vs SHE on the first reductive scan, and i_∞ was measured at the vertex potential on scan 25.

magnitudes of Δf and Δd, attributed to slower relaxation and resulting dehydration.[23] Final frequency and dissipation values of the adsorbed layers are designated Δf_∞ and Δd_∞ and were taken as the values after electrochemical measurements were recorded.

The QCM responses for adsorption of *Mv*BOx on a 3MPA-coated sensor are shown in Figure 2; comparable data for bare gold are shown in the Supporting Information. Once the adsorption process entered stage 4 (5−10 min after adsorption began), cyclic voltammetry (CV) measurements were started to assay the bioelectrocatalytic activity of the protein film (discussed later). Cycling the potential caused oscillations in both frequency and dissipation traces.

The surface coverage increased monotonically with increasing concentration of *Mv*BOx on both bare gold and

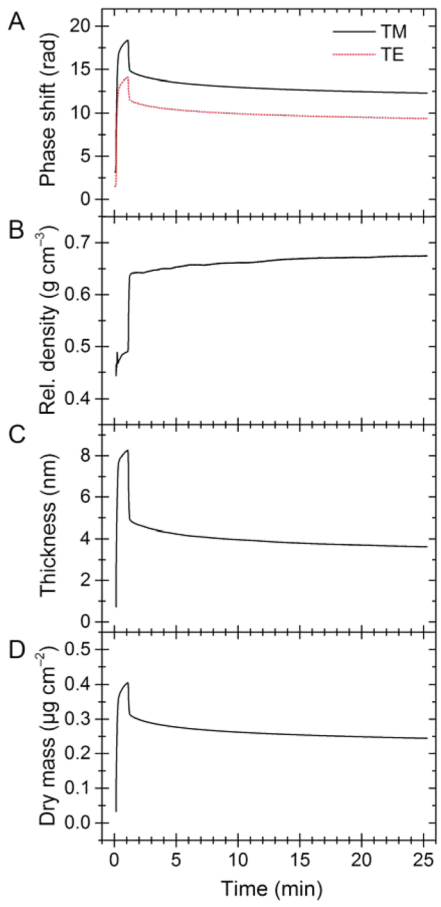

Figure 6. Typical *Mv*BOx adsorption to an unmodified silicon oxynitride DPI sensor. (A) Phase shift, (B) resolved data for density, (C) thickness, and (D) adsorbed dry mass. Conditions: 0.1 M sodium phosphate buffer, pH 6.0, at 25 °C flowing at 0.05 mL min^{-1}; injection: 50 μL of 15 mg mL^{-1} *Mv*BOx.

carboxylate-terminated surfaces (Figure 3A). A saturated monolayer of *Mv*BOx will produce a frequency shift of ca. 300 Hz for the seventh harmonic of a 5 MHz resonator,[8] so surfaces formed from the two highest concentration solutions (25 and 50 mg mL^{-1}) likely have greater than monolayer

DOI: 10.1021/acsami.5b07290
ACS Appl. Mater. Interfaces 2015, 7, 25270−25280

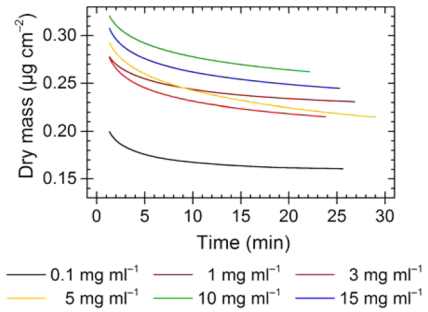

Figure 7. Resolved adsorbed mass DPI data for *Mv*BOx adsorbed onto silicon oxynitride DPI sensors. Conditions: 0.1 M sodium phosphate buffer, pH 6.0, at 25 °C; flow rate 0.05 mL min^{-1}; injection 50 μL of *Mv*BOx.

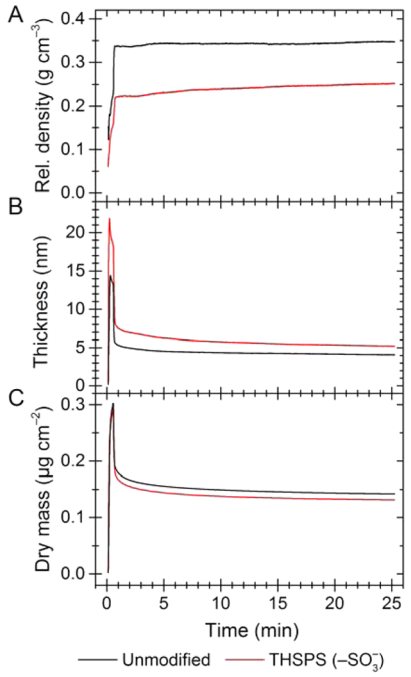

Figure 8. Comparison of *Mv*BOx adsorption on bare and sulfonate-terminated silicon oxynitride DPI sensor: (A) resolved density, (B) thickness, and (C) adsorbed mass. Conditions: 0.1 M sodium phosphate buffer, pH 6.0, at 25 °C flowing at 0.05 mL min^{-1}; injection: 25 mg mL^{-1}*Mv*BOx, 25 μL.

coverage. This is supported by the "overshoot" spike in Δd_{max} (Figure 3B) for these concentrations.[5] The "normalized" dissipation ($\partial d/\partial f$) increased with the deposition solution concentrations above 10 mg mL^{-1} for adsorption stages 1 and 2 on 3MPA-coated surfaces (Figure 3C,D), whereas unmodified gold surfaces only showed a concentration dependence for adsorption stage 2. Longer contact times showed similar frequency or dissipation responses for maximum or final layers

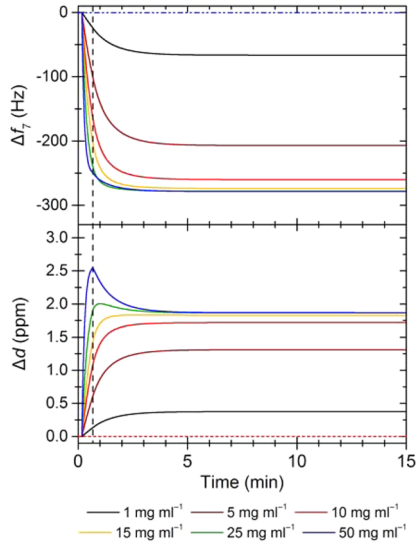

Figure 9. Simulated frequency and dissipation response from protein absorption onto a QCM sensor surface. The model includes an initial 10 s baseline where just buffer is present, the solution is then changed to a protein solution for 30 s before the solution is changed back to buffer (black dashed line), and the concentration of the enzyme in the bulk solution decreases as a first-order exponential with a time constant of 60 s. The properties of the layer are adlayer viscosity 3.2 × 10^{-3} Pa s; adlayer shear modulus 3.2 × 10^5 Pa; adlayer density 1450 kg m^{-3}; fundamental frequency 4.95 MHz; solution density 1.0 × 10^3 kg m^{-3}; and solution viscosity 8.5 × 10^{-4} Pa s.

for concentrations on both 3MPA and gold (Supporting Information).

For a given protein concentration, the magnitude of $\partial d/\partial f$ was always lower for the first stage of adsorption than for the second, consistent with the formation of an rigid layer initially. Higher protein solution concentrations produced less rigid adlayers in stage 1. At lower concentrations, the adsorbed protein has time to relax on the surface and form a more rigid layer. As the solution concentration is increased, the rate of adsorption will also increase, therefore reducing the amount of enzyme relaxation due to neighboring protein electrostatic repulsion and steric hindrance.[18] *Mv*BOx has a pI of around 4.1, so at pH 6, it will have net negative charge.[43] Electrostatic repulsion between the adsorbing macromolecules could reduce the rate surface spreading, particularly at higher surface coverage values.

Effect of MvBOx Concentration on Specific Activity. To assess the mass-specific oxygen reduction activity for *Mv*BOx films formed in the E-QCM-D, CV was performed for 25 scans between 0.31 and 0.91 V vs SHE. The potential sweep in CV measurements has been shown to destabilize adlayers of *Mv*BOx and was used here to quickly reach a steady QCM-D response.[8] A comparison of first CV scan for *Mv*BOx adsorbed onto unmodified and 3MPA-coated sensors is shown in Figure

Table 1. DPI Data Fitted to a Single Exponential Decay for *Mv*BOx Adsorbed on Bare and Sulfonate-Modified Silicon Oxynitride Sensors[a]

modifier	ρ_0 (g cm^{-3})	$\Delta\rho$ (g cm^{-3})	τ_ρ (s)	h_0 (nm)	Δh (nm)	τ_h (s)	m_0 (μg cm^{-2})	Δm (μg cm^{-2})	τ_m (s)
unmodified	0.33	+0.01	82	4.82	−0.72	442	0.16	−0.02	427
THSPS (−SO$_3^-$)	0.22	+0.03	630	6.87	−1.66	417	0.15	−0.02	381

[a]The subscript 0 is the value 120 s after injection, Δ represents the difference between that value and its extrapolated value at infinite time, and τ gives the exponential time constant for the change.

DOI: 10.1021/acsami.5b07290
ACS Appl. Mater. Interfaces 2015, 7, 25270−25280

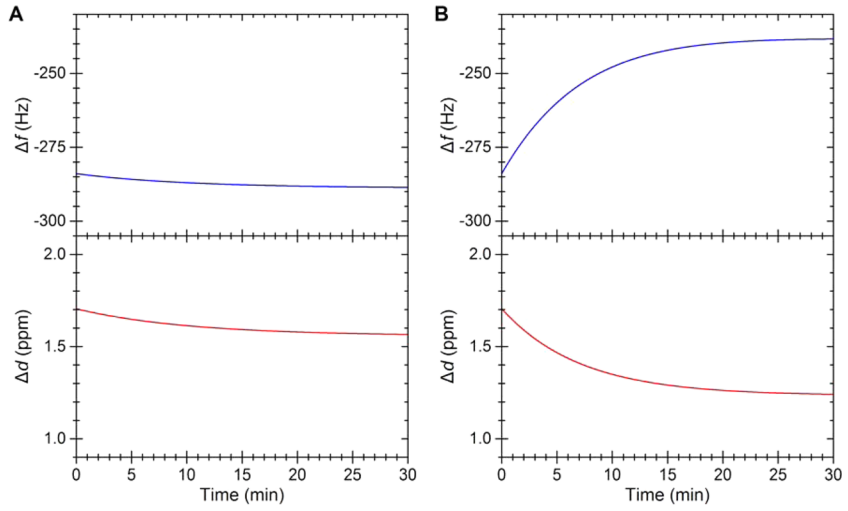

Figure 10. Simulated frequency and dissipation responses from a QCM-D that would result from the thinning of an absorbed protein layer like that generated from a 15 mg mL^{-1} solution of *Mv*BOx. The adlayer viscosity and shear modulus remain constant. (A) Response where the surface protein concentration remains constant (i.e., adlayer thinning is matched by densification). (B) Response when thinning is accompanied by mass loss. Adlayer changes are modeled as first-order exponentials. Adlayer properties: viscosity 3.2 × 10^{-3} Pa s; shear modulus 3.16 × 10^{5} Pa; initial density 1450 kg m^{-3}; final density 1595 kg m^{-3}; densification time constant 660 s; initial thickness 6 × 10^{-9} m; final thickness 4.5 × 10^{-9} m; thickness time constant 440 s; fundamental frequency 4.95 MHz; solution density 1 × 10^{3} kg m^{-3}; solution viscosity 8.5 × 10^{-4} Pa s.

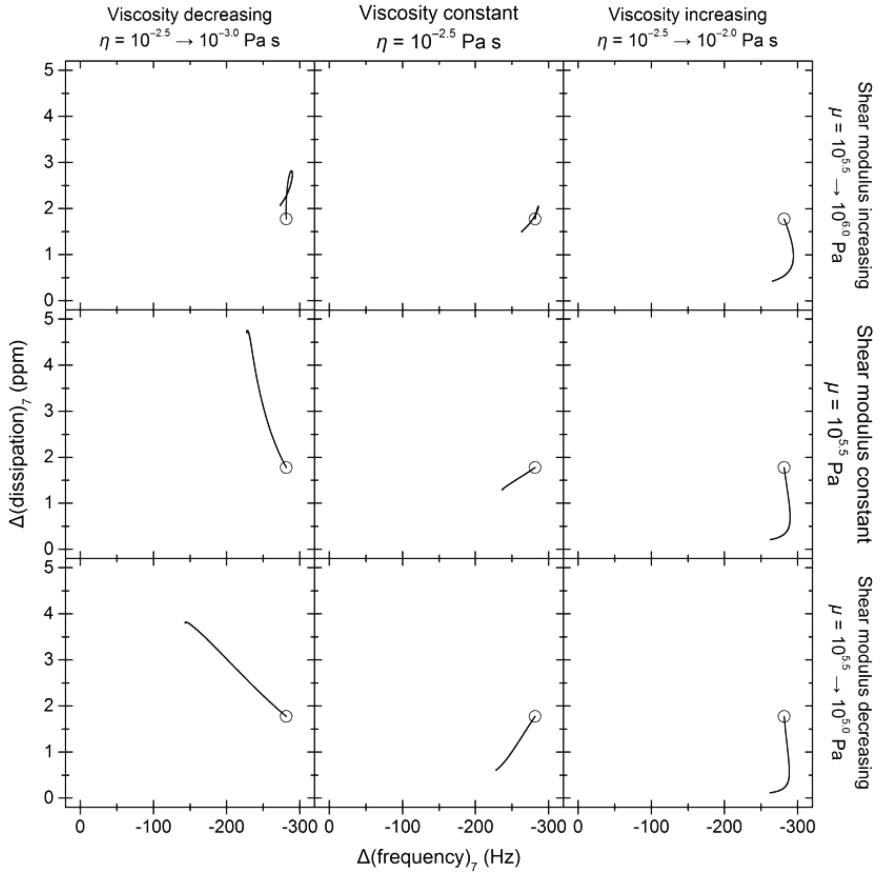

Figure 11. Simulated Δd vs Δf plots for an absorbed and densifying protein layer on a QCM sensor surface undergoing physical property changes during adsorption stages 3 and 4. The circle shows the starting response. In all simulations, the layer undergoes a 25% thickness reduction (τ_h = 440 s) and a density 10% increase (τ_ρ = 660 s) consistent with the DPI analysis of an adlayer formed from 15 mg mL^{-1} *Mv*BOx. The graphs in the left column have a decreasing viscosity (τ_η = 250 s) by a factor of $10^{0.5}$ during the simulation, the center column graphs have a constant viscosity, and the graphs in the right column have an increasing viscosity during the simulation by a factor of $10^{0.5}$. The rows follow a similar trend with shear values increasing or decreasing (τ_μ = 250 s) by a factor of $10^{0.5}$ ordered in rows. The plots show the response for the seventh harmonic. The starting properties of the adlayer are viscosity 3.16 × 10^{-3} Pa s; shear modulus 3.16 × 10^{5} Pa; density 1450 kg m^{-3}; thickness 6 nm; fundamental frequency 4.95 MHz; solution density 1 × 10^{3} kg m^{-3}; solution viscosity 8.5 × 10^{-4} Pa s.

DOI: 10.1021/acsami.5b07290
ACS Appl. Mater. Interfaces 2015, 7, 25270−25280

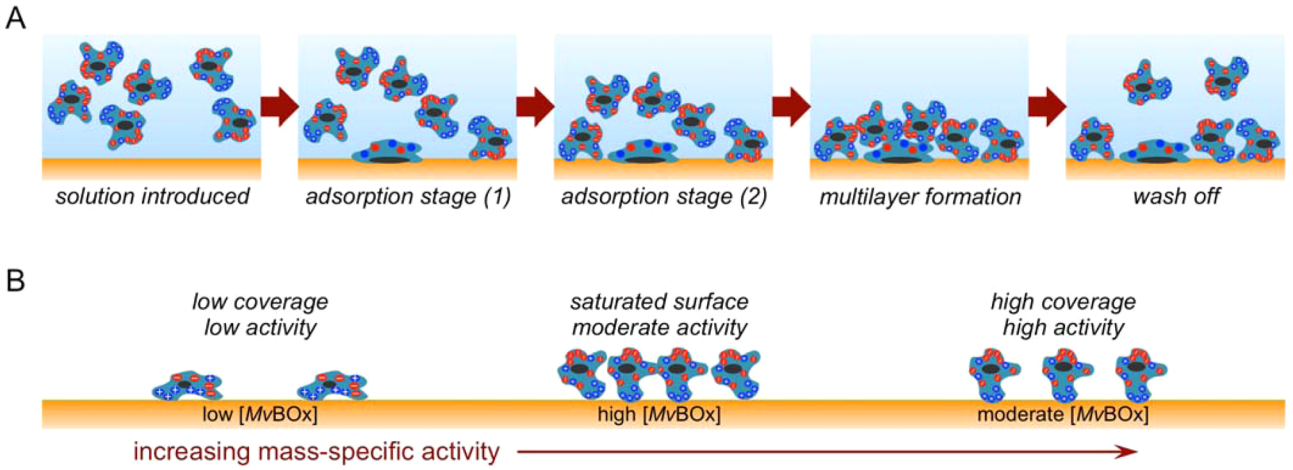

Figure 12. Suggested models for *Mv*BOx interactions with electrode surfaces and their relation to activity at pH 6.0. (A) Two-stage adsorption process. (B) Summary of how the enzyme concentration affects mass-specific catalytic activity.

4. *Mv*BOx activity is proportional to the reductive (negative) current (eq 2). Scans were started from a high (oxidizing) potential where there is not enough driving force for the electron transfer to the copper ions in the enzyme, so no activity is seen. At ca. 0.7 V, enzyme-catalyzed O_2 reduction starts to occur, and the current magnitude increases. This current increases with increasing driving force (lower potentials) until processes such as mass transport limit the reaction rate. For the CV scans in Figure 4A, the concentration of O_2 near the surface is depleted enough to cause the magnitude of the reductive current to peak around 0.55 V and preclude the reverse (oxidative) scan from overlapping with the scan in the reductive direction. Increasing the buffer flow rate by 150% to reduce these mass-transport limitations produced a more sigmoidal response (Supporting Information). Lowering the scan rate from 10 mV s^{-1} to 2 mV s^{-1} did not change the onset potential for electrocatalysis (Supporting Information). The catalytic current at 0.55 V vs SHE was typically about 5−10% higher for the most active protein adlayers.

The activity of the *Mv*BOx adlayer dropped monotonically with each scan (Supporting Information). The plots in the top panels of Figure 5 show how the stability of the protein films decays over about 50 min by comparing the highest magnitude current from the first scan (i_{max}) and that from the 25th scan (i_∞). The most *persistent* (i.e., highest i_∞/i_{max}) catalytic activity was observed on both unmodified gold and 3MPA-coated surfaces from adlayers formed from 15 mg mL^{-1} solutions.

The most *efficient* use of enzyme (i.e., highest mass-specific activity) was determined by taking the ratio of current to frequency change (eq 3). For both initial and final layers, the highest relative turnover frequency is seen to be 15 mg mL^{-1} (Figure 5, bottom panels). A value of 1 μA Hz^{-1} for $i/\Delta f$ corresponds to a turnover frequency of about 90 s^{-1} for this enzyme, so the maximum observed k_{cat} for O_2 reduction was about 60 s^{-1}. This rate is larger than values from solution-based measurements (ca. 15 s^{-1})[7] but is below those obtained for *Mv*BOx adsorbed on a rotating disc electrode (ca. 300 s^{-1}),[12,44] which allowed mass-transport limitations to be factored out. A similar optimum concentration was observed for the specific activity for *Mv*BOx adsorbed onto gold (Supporting Information), but both absolute and mass-specific activity were twice as high for *Mv*BOx adsorbed on 3MPA. Longer protein contact times show a reduction in overall specific activity per adsorbed mass unit yet still give maximum activity per adsorbed mass at a concentration 15 mg mL^{-1}.

Normalized plots that correlate activity and adsorbed mass (Supporting Information) show that films formed from 15 mg mL^{-1} solutions have the lowest activity loss per adsorbed enzyme regardless of surface. The activity of enzyme on unmodified gold surfaces decayed more quickly and to a lower value than 3MPA-coated surfaces.

The mass loss from protein desorption has previously been shown not to be the main cause for loss of bioelectrocatalytic activity.[8] The changes in activity from increasing the concentration appear to be a result of how the enzyme adsorbs and is positioned on the surface, consistent with Welland's model.[33,34] We hypothesize that the adlayer formed at an optimum concentration results in a adsorbed layer that is not overcome by steric hindrance from too much adsorbed material but equally has not had time to form a relaxed state on the surface because of an optimal surface coverage. It may be that some deformation is required on adsorption to produce efficient electron transfer, leading to a drop in specific activity under higher-concentration deposition conditions when the deposition is faster than the rate of surface spreading.

Dual Polarization Interferometry Analysis. DPI measurements of enzyme adsorption from 0.1−15 mg mL^{-1} *Mv*BOx solutions were carried out to independently measure thickness and density changes of the adsorbing layers. The results from a typical DPI measurement for *Mv*BOx adsorbed on a silicon oxynitride sensor are shown in Figure 6. At pH 6, the sensors' silicon oxynitride surface has a surface potential of about −50 mV,[45] giving a surface that is electrically similar to the negatively charged 3MPA-coated surface used for QCM measurements. Yazdanian and co-workers measured surface potentials of −285 mV for carboxylate-terminated SAMs at pH 6 and 0.01 M ionic strength,[46] so it is likely that the 3MPA-coated surface has a higher surface potential, even with an ionic strength more than 10 times higher.[47]

Upon injection of protein, a large phase shift is seen in both polarizations (Figure 6A). This response reflects both the protein adsorption, and the bulk effects of the concentrated protein solution. After injection, the protein sample is then flushed out of the sensor chamber, and a sharp decrease is seen as the solution returns to the bulk buffer. After this point the phase shift decreased, indicating layer thinning, and the

DOI: 10.1021/acsami.5b07290
ACS Appl. Mater. Interfaces 2015, 7, 25270−25280

refractive index increased, indicating layer densification (Figure 6B,C). The density values are those of the protein in the absence of buffer, so they are below 1 g cm^{-3}.[48] The dry mass of the layer also decreases with time (Figure 6D), indicating that some desorption was also occurring.

DPI data for films formed from six concentrations of *Mv*BOx was collected. The resolved adsorbed mass data is shown in Figure 7. The data for density, thickness, and mass were fitted to a first-order exponential decay (Supporting Information). Adlayers from *Mv*BOx solutions with concentrations of 1 mg mL^{-1} and above showed no trends in surface density, thickness, or rate of mass loss. The time constants for changes in these parameters was on the order of hundreds of seconds. The film formed from the 0.1 mg mL^{-1} solution was distinctly thinner and denser than the others, suggesting extensive denaturation of "soft" *Mv*BOx consistent with observations from other soft proteins.[34] The DPI results are also consistent with our hypothesis that films from soft enzymes are less likely to be denatured when the rate of adsorption is higher than the rate at which the protein spreads on the surface.

The DPI response from *Mv*BOx adsorbed on bare and THSPS-modified DPI sensors is shown in Figure 8. The sensors' responses after 120 s were fit to a single exponential decay, with the best-fit parameters tabulated in Table 1. Bare sensors produced denser layers than sulfonate-terminated ones. The density of the *Mv*BOx adlayer on a DPI sensor with no silane modification was about 60% higher than those previously reported for BSA under the same conditions,[34] despite using a similar protocol for surface preparation.[33]

Modeling Adsorption Behavior. We modeled the QCM-D response of the protein adsorption and layer evolution to discover how bulk solution properties might affect some of the sensor response and to determine whether the densification and mass loss observed in the DPI measurements on *Mv*BOx on THSPS would match the QCM responses we observed. First, we aimed to replicate the "overshoot" in Δf and Δd in adsorption stages 1 and 2 (cf. Figure 1) at protein concentrations greater than 5 mg mL^{-1}. These responses are affected by changes in the viscosity and density of the bulk solution. The model response for the seventh harmonic as a function of protein concentration is shown in Figure 9, which is based on experimental conditions similar to those used in Figure 2. The simulations assume irreversible adsorption with no change in mechanical properties after formation and thus does not create two distinct adsorption regions in the Δd versus Δf plots. The model also assumes a continuous homogeneous film rather than one comprised of discrete macromolecular protrusions.

The simulation produced a small overshoot only on the Δd_7 trace for the 25 and 50 mg mL^{-1} solutions. None of the traces shows an overshoot on the Δf_7 trace, suggesting that some of the overshoot may be due to the formation of additional layers of weakly and reversibly bound protein or to the components of the partly formed layers rocking or sliding.[49,50] However, surfaces covered with a submonolayer of rocking micrometer-scale particles produce a positive frequency shift, in contrast with the more negative response observed here.[49] Interestingly, the magnitude of Δf_7 was predicted to increase slightly after the protein slug left the chamber (Supporting Information), a subtle effect that was not observed experimentally. The only way to duplicate the decrease in the magnitude of Δf_7 was by including mass loss in the model (Figure 10).

Figure 11 shows modeled QCM-D responses to changes in an adlayer's viscosity and shear modulus in regions 3 and 4. These models include the changes in density and thickness measured by DPI. The shape of the Δd versus Δf traces with increasing layer viscosity most closely matches the shape of regions 3 and 4 shown in Figure 1B but does not indicate how the shear modulus is changing with time.

Model for Adlayer Evolution and Competence. Figure 12 visually summarizes the formation and evolution of *Mv*BOx adlayers on electrode surfaces. Adsorption followed a two-stage process beginning with the formation of a more rigid layer attributed to spreading, then proceeding to a point where the macromolecules were sterically or electrically restricted from spreading and formed a less rigid layer. Some loosely bound protein washed off from films formed from concentrations above about 10 mg mL^{-1}. The effect of concentration on adsorption to these surfaces showed that the optimum conditions limited surface spreading but did not crowd proteins so much that their activity was affected by mass-transport or electron-transfer limitations.

CONCLUSIONS

This work demonstrated how the combination of electrochemical assays of enzyme activity concurrent with QCM-D measurements provides a route to the most efficient use of immobilized enzymes for industrial biotechnology processes. *Mv*BOx adsorption on bare gold and 3MPA-modified surfaces from 15 mg mL^{-1} solutions at pH 6.0 produced the largest specific electrocatalytic activity for the adlayer. This optimum concentration emerged from a balance between rates of adsorption, reorientation, and unfolding for the protein on the basis of analyses of E-QCM-D and DPI responses to variations in protein concentration and surface chemistry. All the protein adlayers became thinner, denser, less massive, and more viscous after adsorption.

ASSOCIATED CONTENT

Supporting Information

The Supporting Information is available free of charge on the ACS Publications website at DOI: 10.1021/acsami.5b07290.

Modified flow module, adsorption onto 3MPA and bare gold, activity loss with potential cycling, catalytic cyclic voltammetry traces at varied scan rates and pump flow rates, normalized current to frequency response for different *Mv*BOx concentrations on bare gold and 3MPA-coated QCM sensors, longer protein solution contact times, viscosity measurements, additional results from Kelvin–Voigt modeling. (PDF)

AUTHOR INFORMATION

Corresponding Author

*E-mail: christopher.blanford@manchester.ac.uk.

Author Contributions

T.M. collected all the experimental results for the initial submission of the manuscript and wrote early drafts of the manuscript with input from C.F.B. F.F. and T.P.M. collected EQCM-D data for the revised submission. T.P.M. modeled the QCM-D responses. K.S. designed the modified E-QCM-D flow cell. C.F.B. guided the experimental work and edited the final version of the manuscript.

Notes

The authors declare no competing financial interest.

DOI: 10.1021/acsami.5b07290
ACS Appl. Mater. Interfaces 2015, 7, 25270−25280

■ ACKNOWLEDGMENTS

This research was funded by the UK's Engineering and Physical Sciences Research Council (EPSRC) through grant EP/G00434X/2, the NOWNANO Centre for Doctoral Training (T.M.), and the University of Manchester's School of Materials' Doctoral Training Account (T.P.M.). We are grateful to Marcus Swann for valuable discussions on DPI and to Nicola Tirelli for use of his viscometer. In accordance with EPSRC guidelines, the data and flow cell drawing associated with the paper are openly available from The University of Manchester eScholar Data Repository: http://dx.doi.org/10.15127/1.269983 (experimental data) and http://dx.doi.org/10.15127/1.269975 (flow cell CAD file). The computer code associated with this paper is available from Github: http://dx.doi.org/10.5281/zenodo.32859.

■ REFERENCES

(1) Leech, D.; Kavanagh, P.; Schuhmann, W. Enzymatic Fuel Cells: Recent Progress. *Electrochim. Acta* **2012**, *84*, 223−234.
(2) Heller, A.; Feldman, B. Electrochemical Glucose Sensors and Their Applications in Diabetes Management. *Chem. Rev.* **2008**, *108*, 2482−2505.
(3) Norde, W.; Zoungrana, T. Surface-Induced Changes in the Structure and Activity of Enzymes Physically Immobilized at Solid/Liquid Interfaces. *Biotechnol. Appl. Biochem.* **1998**, *28*, 133−143.
(4) van der Veen, M.; Stuart, M. C.; Norde, W. Spreading of Proteins and Its Effect on Adsorption and Desorption Kinetics. *Colloids Surf., B* **2007**, *54*, 136−142.
(5) Rabe, M.; Verdes, D.; Seeger, S. Understanding Protein Adsorption Phenomena at Solid Surfaces. *Adv. Colloid Interface Sci.* **2011**, *162*, 87−106.
(6) Olejnik, P.; Palys, B.; Kowalczyk, A.; Nowicka, A. M. Orientation of Laccase on Charged Surfaces. Mediatorless Oxygen Reduction on Amino- and Carboxyl-Ended Ethylphenyl Groups. *J. Phys. Chem. C* **2012**, *116*, 25911−25918.
(7) Pankratov, D.; Sotres, J.; Barrantes, A.; Arnebrant, T.; Shleev, S. Interfacial Behavior and Activity of Laccase and Bilirubin Oxidase on Bare Gold Surfaces. *Langmuir* **2014**, *30*, 2943−2951.
(8) Singh, K.; McArdle, T.; Sullivan, P. R.; Blanford, C. F. Sources of Activity Loss in the Fuel Cell Enzyme Bilirubin Oxidase. *Energy Environ. Sci.* **2013**, *6*, 2460−2464.
(9) Mano, N.; Soukharev, V.; Heller, A. A Laccase-Wiring Redox Hydrogel for Efficient Catalysis of O_2 Electroreduction. *J. Phys. Chem. B* **2006**, *110*, 11180−11187.
(10) Blanford, C. F.; Foster, C. E.; Heath, R. S.; Armstrong, F. A. Efficient Electrocatalytic Oxygen Reduction by the 'Blue' Copper Oxidase, Laccase, Directly Attached to Chemically Modified Carbons. *Faraday Discuss.* **2009**, *140*, 319−335.
(11) Mano, N.; Edembe, L. Bilirubin Oxidases in Bioelectrochemistry: Features and Recent Findings. *Biosens. Bioelectron.* **2013**, *50*, 478−485.
(12) dos Santos, L.; Climent, V.; Blanford, C. F.; Armstrong, F. A. Mechanistic Studies of the 'Blue' Cu Enzyme, Bilirubin Oxidase, as a Highly Efficient Electrocatalyst for the Oxygen Reduction Reaction. *Phys. Chem. Chem. Phys.* **2010**, *12*, 13962−13974.
(13) Salaj-Kosla, U.; Pöller, S.; Schuhmann, W.; Shleev, S.; Magner, E. Direct Electron Transfer of Trametes Hirsuta Laccase Adsorbed at Unmodified Nanoporous Gold Electrodes. *Bioelectrochemistry* **2013**, *91*, 15−20.
(14) Solomon, E. I.; Sundaram, U. M.; Machonkin, T. E. Multicopper Oxidases and Oxygenases. *Chem. Rev.* **1996**, *96*, 2563−2605.
(15) Page, C. C.; Moser, C. C.; Chen, X. X.; Dutton, P. L. Natural Engineering Principles of Electron Tunnelling in Biological Oxidation-Reduction. *Nature* **1999**, *402*, 47−52.
(16) Gray, H. B.; Winkler, J. R. Long-Range Electron Transfer. *Proc. Natl. Acad. Sci. U. S. A.* **2005**, *102*, 3534−3539.
(17) Norde, W. Adsorption of Proteins from Solution at the Solid-Liquid Interface. *Adv. Colloid Interface Sci.* **1986**, *25*, 267−340.
(18) Herrera, E.; Giacomelli, C. E. Surface Coverage Dictates the Surface Bio-Activity of D-Amino Acid Oxidase. *Colloids Surf., B* **2014**, *117*, 296−302.
(19) Prime, K. L.; Whitesides, G. M. Self-Assembled Organic Monolayers - Model Systems for Studying Adsorption of Proteins at Surfaces. *Science* **1991**, *252*, 1164−1167.
(20) Vallee, A.; Humblot, V.; Al Housseiny, R.; Boujday, S.; Pradier, C. M. BSA Adsorption on Aliphatic and Aromatic Acid SAMs: Investigating the Effect of Residual Surface Charge and Sublayer Nature. *Colloids Surf., B* **2013**, *109*, 136−142.
(21) Tominaga, M.; Ohtani, M.; Taniguchi, I. Gold Single-Crystal Electrode Surface Modified with Self-Assembled Monolayers for Electron Tunneling with Bilirubin Oxidase. *Phys. Chem. Chem. Phys.* **2008**, *10*, 6928−6934.
(22) Ulyanova, Y.; Babanova, S.; Pinchon, E.; Matanovic, I.; Singhal, S.; Atanassov, P. Effect of Enzymatic Orientation through the Use of Syringaldazine Molecules on Multiple Multi-Copper Oxidase Enzymes. *Phys. Chem. Chem. Phys.* **2014**, *16*, 13367−13375.
(23) Singh, K.; Blanford, C. F. Electrochemical Quartz Crystal Microbalance with Dissipation Monitoring: A Technique to Optimize Enzyme Use in Bioelectrocatalysis. *ChemCatChem* **2014**, *6*, 921−929.
(24) Hook, F.; Kasemo, B.; Nylander, T.; Fant, C.; Sott, K.; Elwing, H. Variations in Coupled Water, Viscoelastic Properties, and Film Thickness of a Mefp-1 Protein Film During Adsorption and Cross-Linking: A Quartz Crystal Microbalance with Dissipation Monitoring, Ellipsometry, and Surface Plasmon Resonance Study. *Anal. Chem.* **2001**, *73*, 5796−5804.
(25) Rodahl, M.; Hook, F.; Fredriksson, C.; Keller, C. A.; Krozer, A.; Brzezinski, P.; Voinova, M.; Kasemo, B. Simultaneous Frequency and Dissipation Factor QCM Measurements of Biomolecular Adsorption and Cell Adhesion. *Faraday Discuss.* **1997**, *107*, 229−246.
(26) Höök, F.; Rodahl, M.; Kasemo, B.; Brzezinski, P. Structural Changes in Hemoglobin During Adsorption to Solid Surfaces: Effects of pH, Ionic Strength, and Ligand Binding. *Proc. Natl. Acad. Sci. U. S. A.* **1998**, *95*, 12271−12276.
(27) Swann, M. J.; Peel, L. L.; Carrington, S.; Freeman, N. J. Dual-Polarization Interferometry: An Analytical Technique to Measure Changes in Protein Structure in Real Time, to Determine the Stoichiometry of Binding Events, and to Differentiate between Specific and Nonspecific Interactions. *Anal. Biochem.* **2004**, *329*, 190−198.
(28) Cross, G. H.; Reeves, A. A.; Brand, S.; Popplewell, J. F.; Peel, L. L.; Swann, M. J.; Freeman, N. J. A New Quantitative Optical Biosensor for Protein Characterisation. *Biosens. Bioelectron.* **2003**, *19*, 383−390.
(29) Caruso, F.; Furlong, D. N.; Kingshott, P. Characterization of Ferritin Adsorption onto Gold. *J. Colloid Interface Sci.* **1997**, *186*, 129−140.
(30) Cowsill, B. J.; Coffey, P. D.; Yaseen, M.; Waigh, T. A.; Freeman, N. J.; Lu, J. R. Measurement of the Thickness of Ultra-Thin Adsorbed Globular Protein Layers with Dual-Polarisation Interferometry: A Comparison with Neutron Reflectivity. *Soft Matter* **2011**, *7*, 7223−7230.
(31) Frost, R.; Jonsson, G. E.; Chakarov, D.; Svedhem, S.; Kasemo, B. Graphene Oxide and Lipid Membranes: Interactions and Nanocomposite Structures. *Nano Lett.* **2012**, *12*, 3356−3362.
(32) Coffey, P. D.; Swann, M. J.; Waigh, T. A.; Mu, Q.; Lu, J. R. The Structure and Mass of Heterogeneous Thin Films Measured with Dual Polarization Interferometry and Ellipsometry. *RSC Adv.* **2013**, *3*, 3316−3324.
(33) Xu, K.; Ouberai, M. M.; Welland, M. E. A Comprehensive Study of Lysozyme Adsorption Using Dual Polarization Interferometry and Quartz Crystal Microbalance with Dissipation. *Biomaterials* **2013**, *34*, 1461−1470.
(34) Ouberai, M. M.; Xu, K.; Welland, M. E. Effect of the Interplay between Protein and Surface on the Properties of Adsorbed Protein Layers. *Biomaterials* **2014**, *35*, 6157−6163.
(35) Thourson, S. B.; Marsh, C. A.; Doyle, B. J.; Timpe, S. J. Quartz Crystal Microbalance Study of Bovine Serum Albumin Adsorption

DOI: 10.1021/acsami.5b07290
ACS Appl. Mater. Interfaces 2015, 7, 25270−25280

onto Self-Assembled Monolayer-Functionalized Gold with Subsequent Ligand Binding. *Colloids Surf., B* **2013**, *111*, 707−712.
(36) Rodgers, C. J.; Blanford, C. F.; Giddens, S. R.; Skamnioti, P.; Armstrong, F. A.; Gurr, S. J. Designer Laccases: A Vogue for High-Potential Fungal Enzymes? *Trends Biotechnol.* **2010**, *28*, 63−72.
(37) Swiss Institute of Bioinformatics. ExPASy - Protparam Tool. http://web.expasy.org/protparam/(accessed July, 31 2015).
(38) Voinova, M. V.; Rodahl, M.; Jonson, M.; Kasemo, B. Viscoelastic Acoustic Response of Layered Polymer Films at Fluid-Solid Interfaces: Continuum Mechanics Approach. *Phys. Scr.* **1999**, *59*, 391−396.
(39) Dixon, M. C. Quartz Crystal Microbalance with Dissipation Monitoring: Enabling Real-Time Characterization of Biological Materials and Their Interactions. *J. Biomol. Technol.* **2008**, *19*, 151−158.
(40) Rodahl, M.; Kasemo, B. Frequency and Dissipation-Factor Responses to Localized Liquid Deposits on a QCM Electrode. *Sens. Actuators, B* **1996**, *37*, 111−116.
(41) Fischer, H.; Polikarpov, I.; Craievich, A. F. Average Protein Density Is a Molecular-Weight-Dependent Function. *Protein Sci.* **2004**, *13*, 2825−2828.
(42) Rabe, M.; Verdes, D.; Rankl, M.; Artus, G. R. J.; Seeger, S. A Comprehensive Study of Concepts and Phenomena of the Nonspecific Adsorption of Beta-Lactoglobulin. *ChemPhysChem* **2007**, *8*, 862−872.
(43) Katano, H.; Uematsu, K.; Hibi, T.; Ikeda, T.; Tsukatani, T. Application of Poly[oxyethylene(dimethylimino)propyl-(dimethylimino)ethylene] as Enzyme Stabilizer for Bilirubin Oxidase Immobilized Electrode. *Anal. Sci.* **2009**, *25*, 1077−1081.
(44) Cracknell, J.; McNamara, T.; Lowe, E.; Blanford, C. F. Bilirubin Oxidase from *Myrothecium verrucaria*: X-Ray Determination of the Complete Crystal Structure and a Rational Surface Modification for Enhanced Electrocatalytic O_2 Reduction. *Dalton Trans.* **2011**, *40*, 6668−6675.
(45) Shovsky, A.; Bijelic, G.; Varga, I.; Makuška, R.; Claesson, P. M. Adsorption Characteristics of Stoichiometric and Nonstoichiometric Molecular Polyelectrolyte Complexes on Silicon Oxynitride Surfaces. *Langmuir* **2011**, *27*, 1044−1050.
(46) Yazdanian, M.; Yu, H.; Zografi, G. Ionic Interactions of Fatty Acid Monolayers at the Air/Water Interface. *Langmuir* **1990**, *6*, 1093−1098.
(47) Noy, A.; Vezenov, D. V.; Lieber, C. M. Chemical Force Microscopy. *Annu. Rev. Mater. Sci.* **1997**, *27*, 381−421.
(48) Escorihuela, J.; González-Martínez, M. Á.; López-Paz, J. L.; Puchades, R.; Maquieira, Á.; Gimenez-Romero, D. Dual-Polarization Interferometry: A Novel Technique to Light up the Nanomolecular World. *Chem. Rev.* **2015**, *115*, 265−294.
(49) Pomorska, A.; Shchukin, D.; Hammond, R.; Cooper, M. A.; Grundmeier, G.; Johannsmann, D. Positive Frequency Shifts Observed Upon Adsorbing Micron-Sized Solid Objects to a Quartz Crystal Microbalance from the Liquid Phase. *Anal. Chem.* **2010**, *82*, 2237−2242.
(50) Johannsmann, D.; Reviakine, I.; Richter, R. P. Dissipation in Films of Adsorbed Nanospheres Studied by Quartz Crystal Microbalance(QCM). *Anal. Chem.* **2009**, *81*, 8167−8176.

DOI: 10.1021/acsami.5b07290
ACS Appl. Mater. Interfaces 2015, 7, 25270−25280